Automotive Science and Engineering, Vol. 15, No. 1, (2025), 4608-4618

Iran University of Science and Technology

Automotive Science and Engineering

Journal Homepage: ase.iust.ac.ir

ISSN: 2008-9899

Numerical simulation of airflow distribution impact on radiator performance in the QUIK automobile

Hojjat Saberinejad[1*]

[1]Assistant professor, Department of Mechanical Engineering, National University of Skills (NUS), Tehran, Iran

ARTICLE INFO

Article history:

Received : 25 Oct 2024

Accepted: 15 Dec 2024

Published: 20 Jan 2025

Keywords:

Numerical study

Radiator performance

Porous media

Darcy number

Forchheimer coefficient

A B S T R A C T

One of the main challenges in designing a vehicle's cooling system, particularly the radiator, is not considering the non-uniform airflow distribution in the radiator's characteristic performance graphs. In this study, a three-dimensional numerical analysis of the airflow passing through a QUIK vehicle and the effect of the cooling system's placement relative to the vehicle's grille in five different cases was conducted. The effect of non-uniform airflow distribution on related radiator parameters such as the Darcy number, particle diameter, and inertial term was examined. The results indicate that the optimal placement range of the vehicle's cooling system for appropriate cooling performance is very limited. Additionally, non-uniform air velocity distribution plays a significant role in the radiator pressure drop. The inertial term is more significant in non-uniform flow conditions. For larger Forchheimer numbers, the change in radiator pressure drop for uniform compared to non-uniform flow distributions is about 22%.

1. Introduction

Enhancing the thermal efficiency of car radiators is one of the most significant technical challenges in automotive cooling. Designing and optimally positioning the radiator in the car's engine compartment involves complex trade-offs among increasing engine thermal and mechanical efficiency, reducing fuel consumption, and lowering overall production costs. Increasing engine thermal efficiency leads to reductions of 1.5–2% in total fuel consumption and decreases of 12% and 16% in carbon monoxide (CO) and hydrocarbon (HC) emissions, respectively [1, 2]. The compression of under-hood arrangements in new automotive design technologies, along with increased engine power and thermal loads, can lead to elevated temperatures of components within the vehicle compartment [3, 4]. This rise in temperature reduces the service life of these components and diminishes vehicle safety [5]. Therefore, effective thermal management is essential to ensure component reliability and overall safety.

The performance characteristics of radiators—specifically, the pressure drop variations relative to the mass flow rate of air—are typically determined under wind tunnel conditions with uniform airflow. However, in real-world scenarios, the effect of non-uniform airflow resulting from passing through the car's grille, intercooler, condenser, and air guides is significant. This discrepancy makes the radiator cooling design process critically important. The placement of the engine, its accessories, gearbox, and cooling system is crucial for optimal component positioning within the engine compartment. Since the incoming airflow passes through several porous media, such as the oil cooler and condenser, before reaching the radiator and enduring significant pressure drops, examining the location and configuration of the cooling system components—including the condenser, radiator, and fan assembly—is essential for achieving suitable air distribution. Despite numerous CFD analyses conducted on the cooling

*Corresponding Author
Email Address: hsaberinejad@nus.ac.ir
https://doi.org/10.22068/ase.2025.692

"*Automotive Science and Engineering*" is licensed under a Creative Commons Attribution-Noncommercial 4.0 International License.

[Downloaded from ase.iust.ac.ir on 2025-04-09]

[DOI: 10.22068/ase.2025.692]

efficiency of automobile radiators [6-10], many studies assume uniform airflow and may not fully account for the complexities introduced by non-uniform airflow and cooling drag at high vehicle speeds.

For instance, Kayastha [11] numerically analyzed an automobile radiator with helical tubes of two different pitches, finding that minimum pressure drop and maximum temperature drop occur at lower mass flow rates in helical-type tubes. Patel et al. [12] investigated radiator performance under various geometric and operating parameters to present optimal configurations. Sekhar et al. [13] examined the effect of different radiator materials on thermal performance at various cooling airflow speeds, calculating coolant flow rates for both copper and aluminum radiators. Zhang et al. [14] analyzed the effect of front and rear component arrangements on the thermal performance of the radiator in the Hyundai Veloster, demonstrating that proper management of cooling airflow patterns can simultaneously improve radiator performance and reduce drag force. David and Kumar [15] studied the effect of helical tubes on heat transfer behavior, showing that heat transfer is enhanced by using helical tubes. Additionally, experimental studies on enhancing heat transfer in radiators have been conducted [16-18]. Although the effects of inertial terms on the pressure drop of uniform fluid flow through porous media are well-known [19-23], applying these results to automotive radiators is unsuitable due to cooling drag and non-uniform airflow through the radiator. At high vehicle speeds, the airflow passing through the bumper grilles, condenser, brackets, radiator, and fan becomes non-uniform. To date, the combined effects of cooling drag and inertial terms on the radiator's pressure drop under these conditions have not been thoroughly investigated.

This study aims to address this gap by conducting a numerical simulation of the QUIK Automatic car at its top speed. We analyze the effect of the projected airflow area on the radiator for five different scenarios. Additionally, we examine how varying the characteristics of the radiator—modeled as a porous medium—such as the Forchheimer coefficient, Darcy number, and particle diameter impact the pressure drop. By evaluating these factors, we seek to optimize radiator design and placement under realistic operating conditions, contributing to enhanced thermal management in modern vehicles.

2. Problem definition

The simulation model of the QUIK car for CFD analysis is shown in Figure 1. Figure 2 displays the change in position of the car's cooling system relative to the car's centerline and its placement against the car's grille. Distances of 10, 15, 35, 40, and 60 millimeters along the ±y axis between the center of the vehicle and the location of the radiator were selected to achieve different ratios of the inlet air surface area to the radiator surface area (β). The values of β for these transverse displacements of the radiator are 0.352, 0.355, 0.342, 0.340 and 0.350, respectively.

For the optimal placement of the radiator against the incoming airflow (optimal β for air velocity distribution on the radiator), the effect of varying the non-uniform airflow on the radiator's pressure drop was analyzed. particle diameter ranges from 0.01 to 1 mm, with three different Forchheimer coefficients of 0.15, 0.3, and 0.5, and three Darcy numbers of $Da = 10^{-6}$, $Da = 10^{-5}$ and $Da = 10^{-4}$.

The geometric specifications and thermal capacities of the car cooling system components are as follows: the radiator measures 65 cm in length, 41 cm in width, and 5 cm in thickness, with a thermal capacity of 30 kW. The condenser measures 73 cm in length, 36 cm in width, and 4 cm in thickness, with a thermal capacity of 12 kW. Lastly, the oil cooler measures 54 cm in length, 15 cm in width, and 4 cm in thickness, with a thermal capacity of 10 kW.

These specifications are based on the experimental data obtained from Saipa Research and Development Center. Figure 3 shows the cooling system and the components inside the car compartment, along with their arrangement.

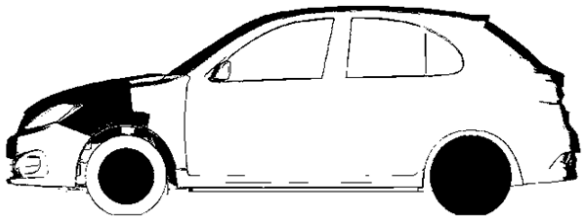

Figure 1: Schematic of QUIK car model.

[Downloaded from ase.iust.ac.ir on 2025-04-09]

[DOI: 10.22068/ase.2025.692]

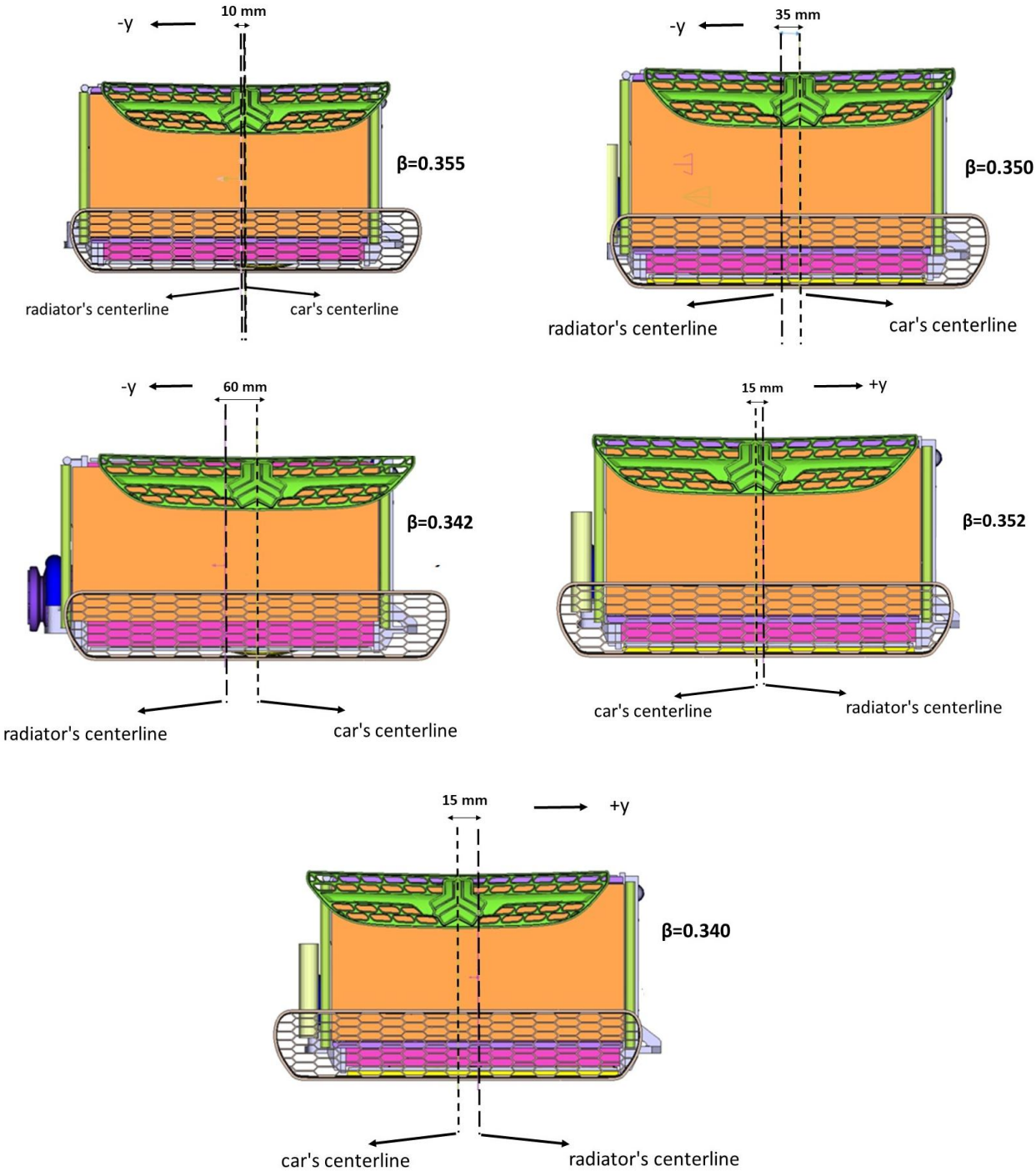

Figure 2: Different positions of the cooling system relative to the car's air intake grille

[Downloaded from ase.iust.ac.ir on 2025-04-09]

[DOI: 10.22068/ase.2025.692]

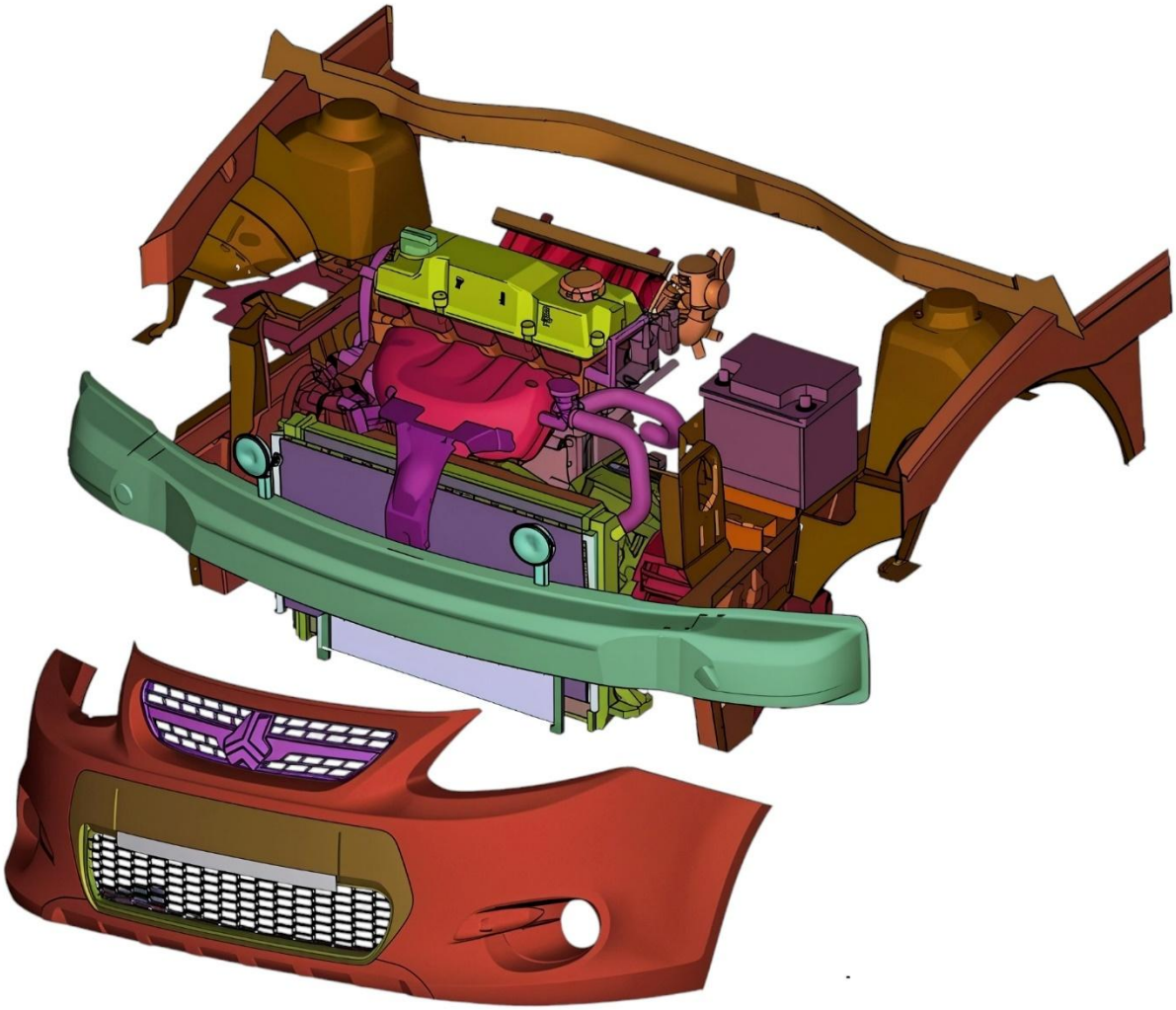

Figure 3: Geometrical simulation of cooling system and the components inside the car compartment

3. Numerical method

The airflow is three-dimensional, and the car was simulated at a speed of 155 km/h. The Navier-Stokes equations and the realizable $k-\varepsilon$ turbulence model were used for the numerical analysis. The Darcy-Brinkman-Forchheimer model was used for simulating the porous medium. The oil cooler, condenser, and radiator were simulated as porous media with the specifications provided in Table 1. Since the governing equations for steady three-dimensional incompressible turbulent flow are well-known [24-26], they are not reiterated here.

Additionally, the non-Darcian model equations for a porous medium are presented in the references [19, 27-30]. The Moving Reference Frame (MRF) approach [31, 32] was used to simulate the airflow in the radiator fan with a rotational speed of 2500 rpm. The MRF approach is a common method to reduce the cost and time of numerical analysis for unsteady industrial moving parts with appropriate accuracy. ANSYS FLUENT 18.1 has been employed to simulate airflow within the vehicle's cooling system. Finite volume method is applied to discrete the governing equations and SIMPLE algorithm is used for coupling the velocity and pressure fields. The discretization of convective, diffusion and pressure terms are conducted by upwind second order, central second order and Presto algorithm respectively. The algebraic equations are implicitly solved by iterative line by line Gauss-Seidel method. Mesh generation done by ANSA 19.1.3 software. Surface meshing of the car model and wind tunnel was performed using a triangular mesh. The structured mesh was applied for surface meshing of the radiator, condenser, and oil cooler. In Figure 4, the surface meshing on the car model and cooling system is shown. A non-uniform HEXA volumetric grid, which is clustered in high gradient regions such as near walls, was generated to ensure a sufficiently fine mesh in the laminar sublayer. The comparison of experimental results and

[Downloaded from ase.iust.ac.ir on 2025-04-09]

[DOI: 10.22068/ase.2025.692]

numerical analysis for pressure drop variations with free airflow velocity in the radiator, specified in Table 1, is shown in Figure 5. The experimental results were conducted at the Saipa Research and Development Center. The comparison indicates that the computational fluid dynamics model has an acceptable agreement with the experimental results. In Table 1, C_1 represents viscous resistance, defined as 1/K, where K denotes permeability (m^2). C_2 is inertia resistance, formulated as ($2F/\sqrt{K}$), where F is the Forchheimer coefficient and ϕ signifies porosity. To examine grid independence, the mass flow rate of air entering the radiator was analyzed for four volumetric grids with dimensions of 25214561; 35412435; 47187632; and 58934564, with growth rates of 1.05, 1.04, 1.03, and 1.02, respectively. Figure 6 indicates that the air mass flow rate over the radiator surface for a computational grid with dimensions greater than 3.55×10^7shows negligible changes. Therefore, the grid with a dimension of 35412435 was selected for numerical analysis. The convergence criterion for the velocity parameters in three directions, turbulent energy and dissipation, and continuity was set to be less than 10^{-6}. The boundary condition at the front face of the wind tunnel is considered as an inlet velocity. The incoming air velocity is constant and equal to the desired vehicle speed (U_0). Road conditions are considered as a moving wall (the speed of the bottom face of the wind tunnel is equal to the desired vehicle speed). The outlet of the virtual wind tunnel is set with a zero gradient along the flow direction. The zero magnitude of specified shear stress is applied for the side walls and top wall of the virtual tunnel. The turbulent intensity and viscosity ratio are assumed 0.1%~0.25% and 200, respectively. The rotational speed of the tires is adjusted based on their diameter and the desired vehicle speed. The rotational speed of the radiator fan is 2500 rpm. These conditions are summarized in Figure 7.

Table 1: Specifications of Three Porous Media in the Vehicle

	C_1: viscous resistance ($1/m^2$)	C_2: inertial resistance ($1/m$)	ϕ : porosity
Radiator	2.84×10^7	206.26	0.98
Condenser	3.75×10^7	311.68	0.97
Oil cooler	4.09×10^7	253.68	1

Figure 4: Surface meshing of car model and cooling system

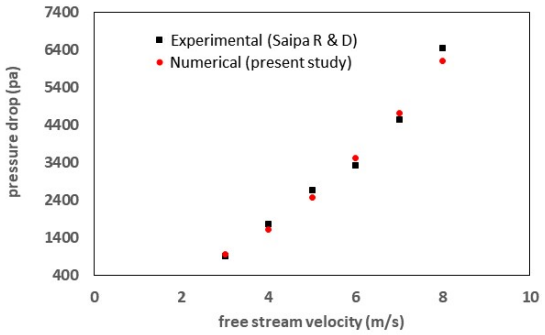

Figure 5: Verification of numerical code: pressure drop versus $\mathbf{u}_\infty$

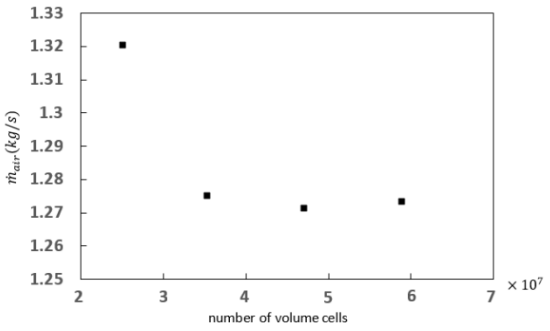

Figure 6: Grid independency of air mass flow rate on the radiator surface

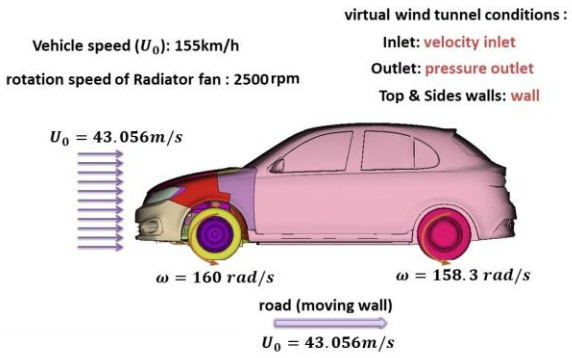

Figure 7: Problem Boundary conditions

[Downloaded from ase.iust.ac.ir on 2025-04-09]

[DOI: 10.22068/ase.2025.692]

4. Results and discussion

Typically, the dimensionless air velocity ($u^* = u/U_0$) distribution and streamlines over the car are shown in Figures 8 and 9. It is evident that the airflow entering the car's engine compartment slows down due to collisions with the bumper and front grille. The impact of various surfaces of the car on the distribution of airflow passing over the vehicle can be observed. The airflow reaching the car radiator becomes non-uniform and slows down due to coolant drag from the components within the engine compartment (Figures 10 and 11).

The dimensionless air velocity vectors over the cooling system and the dimensionless air velocity contours over the car radiator are shown in Figures 10 and 11. The deflection of airflow around the radiator under the influence of the fan is clearly visible. The velocity contour over the radiator is non-uniform due to the components in front of the radiator, which divert the airflow. Figure 11 shows that approximately 15% of the free stream air velocity reaches the radiator. Additionally, due to the obstruction of airflow by various components in front of the radiator, there are regions on the radiator surface where the air velocity is very low, causing the flow in these areas to become nearly stagnant. Based on experimental data from the Saipa Research and Development Center, for proper radiator cooling performance, the average dimensionless air velocity (u^*) should be greater than 0.0375. This criterion is essential for the adequate performance of the car's cooling system under critical conditions, such as driving uphill in the summer with the air conditioning on.

Figure 12 shows the area-weighted average dimensionless air velocity over the radiator and the mass flow rate of air passing through the radiator for the different configurations presented in Figure 2. Therefore, considering Figure 12 and the stated criterion, Only the configuration with β=0.355 is acceptable for adequate cooling performance. Consequently, the importance of the cooling system layout is highlighted, and a very limited range of cooling system displacement is feasible. Since the design and assembly management process of the car's cooling system involves various parameters such as size, type, and technology of the cooling system, understanding the suitable placement range can be a key factor in the proper performance of the car's cooling system.

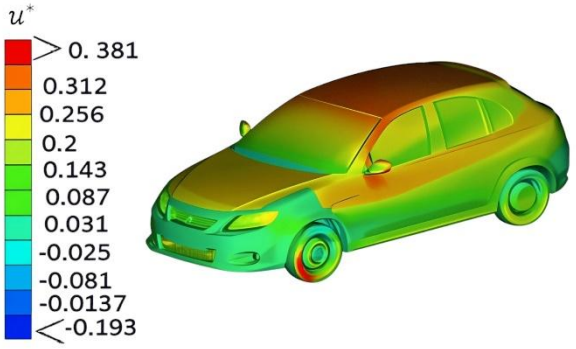

Figure 8: Dimensionless air velocity distribution on the vehicle

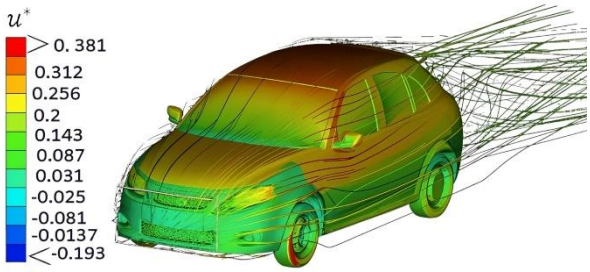

Figure 9: Streamlines colored with dimensionless velocity on the vehicle

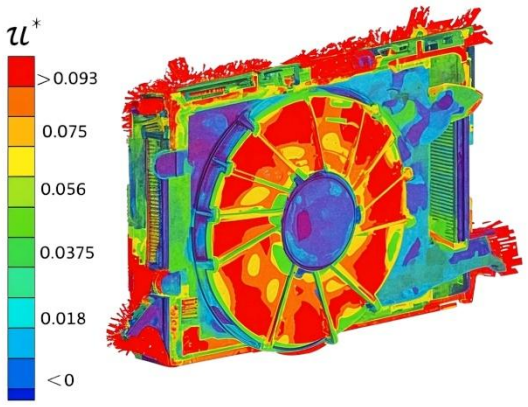

Figure 10: Dimensionless air velocity vectors over the cooling System

[Downloaded from ase.iust.ac.ir on 2025-04-09]

[DOI: 10.22068/ase.2025.692]

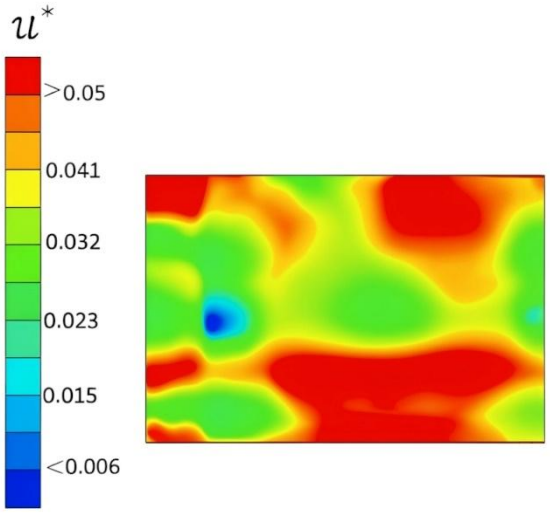

Figure 11: Dimensionless air velocity contour on the radiator

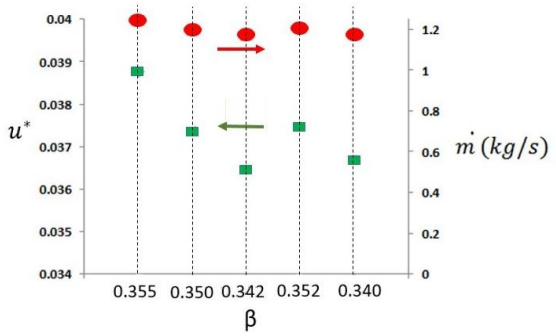

Figure 12: Area-weighted average dimensionless velocity and air mass flow rate on the radiator in different configurations

In continuation of this study, for the optimal configuration with β=0.355, the effect of changes in geometric properties (permeability K and particle diameter d_p) and the inertial term (Forchheimer coefficient F) of the radiator on the pressure drop under non-uniform air distribution conditions has been examined. Performance graphs of the radiator pressure drop based on the airflow velocity passing through it under uniform free airflow are provided, whereas the results of Figures 10 and 11 indicate that in real conditions, this airflow is non-uniform.

The effect of particle diameter in the porous medium (equivalent to the radiator wire mesh screens) on the dimensionless airflow velocities over the radiator in both uniform and non-uniform flow conditions at $\phi = 0.97$, F =0.15 and $Da = 10^{-6}$ is presented in Figure 13. As observed in this figure, at a constant airflow velocity, increasing the particle diameter reduces the pressure drop in the radiator. This is because an increase in the particle diameter in the porous medium, at a constant permeability, reduces the inertial resistance term, resulting in a lower pressure drop [19, 22]. Additionally, the non-uniformity of the airflow has a minimal effect on the pressure drop in the radiator with varying particle diameters in the porous medium (with a maximum difference of about 4%). Therefore, in the radiator design process, the graph of pressure drop changes based on the airflow velocity passing through the part is acceptable for the parameter of the radiator wire mesh screens size (evaluating the characteristic graph for the industrial part alone).

Figure 14 shows the effect of the Darcy number or permeability of the radiator on its pressure drop at various dimensionless airflow velocities over the radiator in both uniform and non-uniform flow conditions for ϕ =0.97, F=0.15, and d_p =0.01mm. This figure indicates that the non-uniformity of the flow has a significant impact on the results. At a lower Darcy number and higher airflow velocities, the difference in pressure drop between uniform and non-uniform conditions becomes more pronounced. This difference is at its maximum, about 12%, for $Da = 10^{-6}$ Additionally, the overall trend of pressure drop variations with airflow velocity follows a similar pattern for both uniform and non-uniform conditions. Therefore, the radiator in the installed condition in the vehicle, in some cases, experiences less pressure drop compared to the characteristic performance graphs. As a result, the cooling efficiency of the radiator will be affected.

The effect of the inertial parameter in the porous medium on the pressure drop at various uniform and non-uniform airflow velocities for ϕ=0.97, d_p = 0.01 mm and two different Darcy numbers is plotted in Figure 15(a and b). This figure indicates that the inertial parameter has the most significant impact on the pressure drop in both uniform and non-uniform airflow distributions. An increase in the Forchheimer coefficient at a given Darcy number results in a higher pressure drop in the radiator, which is more significant at higher airflow velocities. Additionally, the figure shows that the type of airflow distribution over the radiator pressure drop. For instance, the difference in pressure drop for the radiator at $Da = 10^{-6}$ and F =0.5 under uniform and non-uniform airflow at u^* =0.1393 is 15%. In contrast, the pressure drop difference under the same conditions at $Da = 10^{-4}$ is 22%. This implies that the effect of the Forchheimer coefficient (inertia term) in a porous medium depends on whether the flow is uniform or non-uniform. Whereas for uniform flow, it is only dependent on porosity [23, 27].

[Downloaded from ase.iust.ac.ir on 2025-04-09]

[DOI: 10.22068/ase.2025.692]

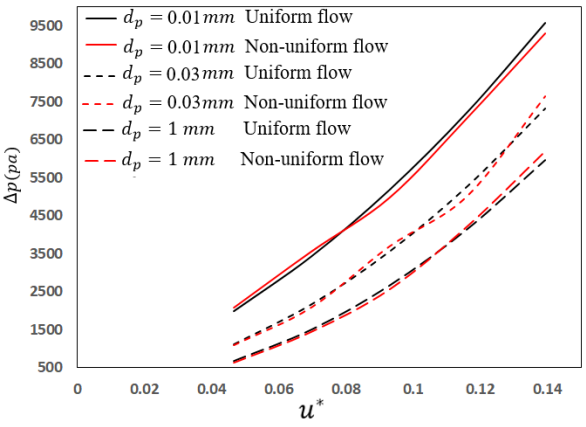

Figure 13: Effect of particle diameter on pressure drop under uniform and non-uniform airflow, ϕ =0.97, F =0.15 and $Da = 10^{-6}$.

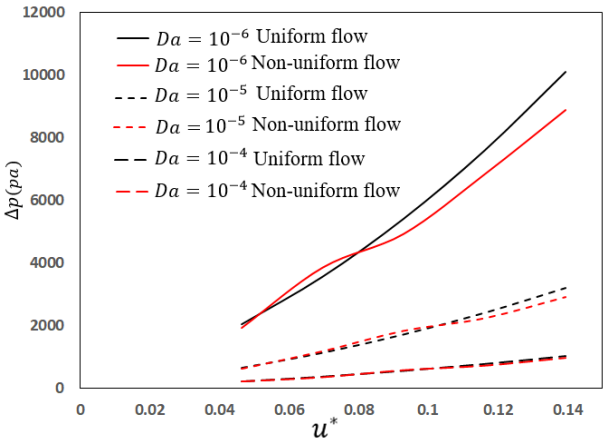

Figure 14: Effect of darcy number on pressure drop under uniform and non-uniform airflow, ϕ =0.97, F =0.15 and d_p =0.01mm.

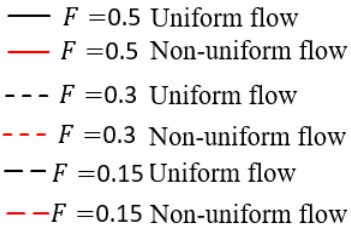

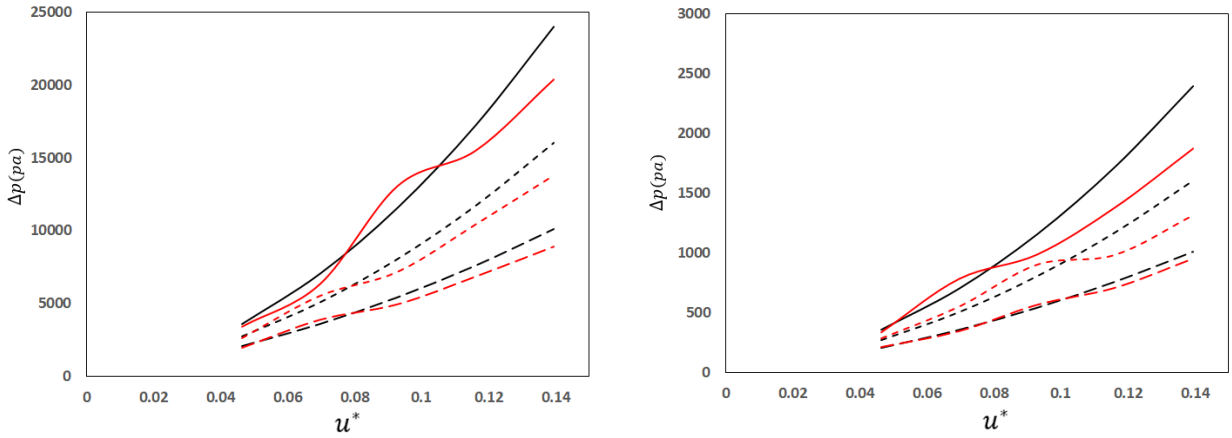

(a) $Da = 10^{-6}$ **(b) $Da = 10^{-4}$**

Figure 15: Effect of Forchheimer coefficient on pressure drop under uniform and non-uniform airflow, ϕ =0.97 and d_p =0.01mm, (a) $Da = 10^{-6}$, (b) $Da = 10^{-4}$.

[Downloaded from ase.iust.ac.ir on 2025-04-09]

[DOI: 10.22068/ase.2025.692]

5. Conclusions

A comprehensive numerical investigation on the three-dimensional airflow distribution across the radiator of a QUIK vehicle was conducted. The optimal placement of the radiator and the effect of pertinent parameters, such as the Darcy number, particle diameter, and Forchheimer coefficient on the radiator pressure drop, were examined. Based on this study, the following conclusions can be drawn:

- To achieve optimal cooling performance in a vehicle, the geometric placement of the cooling system within the engine compartment is constrained.
- The non-uniform airflow over the radiator has a minimal effect on the pressure drop concerning the change in the particle diameter parameter, although for smaller particle diameters, the pressure drop increases in both uniform and non-uniform velocity distributions.
- At lower Darcy numbers, the non-uniformity of the airflow velocity distribution over the radiator has a greater impact on the pressure drop.
- The non-uniform airflow velocity distribution over the radiator has the greatest impact on the inertial parameter compared to changes in the radiator pressure drop.
- For higher Darcy numbers and larger Forchheimer coefficients, the effect of non-uniform airflow distribution on the radiator pressure drop is more significant.
- Designing the vehicle cooling system using performance graphs at the component level can have an adverse impact on the vehicle's cooling performance.

List of symbols

C_1	viscous resistance (m^2)
C_2	inertia resistance ($1/m$)
d_p	Particle diameter (mm)
Da	Darcy number
F	Forchheimer coefficient
k	turbulent kinetic energy per unit mass (m^2/s^2)
K	Permeability (m2)
$\dot{m}$	mass flow rate of air on the radiator (kg/s)
u	velocity in x-direction (m/s)
U_0	desired vehicle speed (m/s)
u^*	dimensionless air velocity, u/U_0

Greek symbols

β	ratio of the inlet air surface area to the radiator surface area
ε	dissipation rate of k (m^2/s^3)
ϕ	porosity

References

[1] A. Torregrosa, A. Broatch, P. Olmeda, and C. Romero, Assessment of the influence of different cooling system configurations on engine warm-up, emissions and fuel consumption, International Journal of Automotive Technology, vol. 9, (2008) pp. 447-458.

[2] F. Thomaz, G. A. R. de Paula, A. C. T. Malaquias, and J. G. C. Baeta, Effects of the engine cooling system design on fuel consumption-A numerical assessment, SAE Technical Paper,(2021)pp. 0148-7191.

[3] M. Khaled, J. Faraj, E. Harika, F. Harambat, C. Castelain, and M. Ramadan, Impact of underhood leakage zones on the aerothermal situation–Experimental simulations and physical analysis, Applied Thermal Engineering, vol. 145, (2018), pp. 507-515.

[4] M. Khaled, F. Harambat, and H. Peerhossaini, Underhood thermal management: Temperature and heat flux measurements and physical analysis, Applied Thermal Engineering, vol. 30, no. 6-7, (2010) pp. 590-598.

[5] A. Broatch, P. Olmeda, J. Martín, and A. Dreif, Improvement in engine thermal management by changing coolant and oil mass,

[Downloaded from ase.iust.ac.ir on 2025-04-09]

[DOI: 10.22068/ase.2025.692]

Applied Thermal Engineering, vol. 212, (2022) p. 118513.

[6] S. Maddipatla, Coupling of CFD and shape optimization for radiator design, Oakland University. Ph. D. thesis, (2001).

[7] S. Sridhara, S. Shankapal, and V. U. Babu, CFD analysis of fluid flow and heat transfer in a single tube-fin arrangement of an automotive radiator, in International Conference on Mechanical Engineering, (2005), pp. 2033-2043.

[8] H. Van der Vyver, J. Dirker, and J. P. Meyer, Validation of a CFD model of a three-dimensional tube-in-tube heat exchanger, in Proc. 3rd International Conference on CFD in the Minerals and Process Industries, (2003), pp. 235-240.

[9] S. Chacko, Numerical Simulation for Improving Radiator Efficiency by Air Flow Optimization, in ANSA & μETA International Congress, (2005), pp. 2-3.

[10] R. Nimtan, A. K. Doost, and N. Madani, Simulation of air flow under the hood of a passenger car using computational fluid dynamics, Research Journal of Applied Sciences, Engineering and Technology, vol. 6, no. 24, (2013) pp. 4583-4594.

[11] K. S. Kayastha, CFD simulation of heat transfer analysis of automobile radiator using helical tubes, International journal of engineering research and development, vol. 11, no. 1, (2015), pp. 24-35.

[12] H. B. Patel, D. Dinesan, H. Patel, and D. Dinesan, Performance analysis of an automobile radiator using CFG, International Journal for Innovative Research in Science & Technology, vol. 1, (2016), pp. 318-322.

[13] R. Sathyan, Analysis of automobile radiator using computational fluid dynamics, International Journal of Latest Technology in Engineering, Management & Applied Science (IJLTEMAS) Volume, vol. 6, (2016).

[14] C. Zhang, M. Uddin, A. C. Robinson, and L. Foster, Full vehicle CFD investigations on the influence of front-end configuration on radiator performance and cooling drag, Applied Thermal Engineering, vol. 130, (2018), pp. 1328-1340.

[15] K. David and A. Kumar, "CFD and heat transfer analysis of automobile radiator using helical tubes," Int. J. Innov. Res. Sci. Eng. Technol.(IJIRSET), vol. 8, no. 5,(2019).

[16] N. A. Ghiasi, M. Baghaeian, and H. R. Goshayeshi, Experimental comparison of heat transfer coefficient and pressure drop of graphene oxide, titanium oxide and aluminum oxide on the radiator of a car, Automotive Science and Engineering, Vol. 13, No. 3, (2023).

[17] M. Fakhari and G. Sheikhzadeh, Heat Transfer and Pressure Drop of Al2O3-Ethylene Glycol-water Nanofluid as the Coolant in an Automotive Radiator, Automotive Science and Engineering, Vol. 10, No. 1, (2020), pp.3188-3201.

[18] S. Oduro, Assessing the effect of blockage of dirt on engine radiator in the engine cooling system, Automotive Science and Engineering, Vol. 2, NO.3, (2012).pp.165-171.

[19] H. Saberinejad, A. Keshavarz, M. Payandehdoost, M. R. Azmoodeh, and A. Batooei, Numerical study of heat transfer performance in a pipe partially filled with non-uniform porous media under LTNE condition, International Journal of Numerical Methods for Heat & Fluid Flow, vol. 28, no. 8, (2018), pp. 1845-1865.

[20] D. Śnieżek, S. B. Naqvi, and M. Matyka, Inertia onset in disordered porous media flow, Physical Review E, vol. 110, no. 4, (2024), p. 045103.

[21] Z. Tian, Y. Huang, and M. Wang, Analytical solution of inertia effect in high-speed flows through disordered porous media, Physical Review Fluids, vol. 9, no. 10, (2024), pp. L102101.

[22] Y. Mahmoudi and N. Karimi, Numerical investigation of heat transfer enhancement in a pipe partially filled with a porous material under local thermal non-equilibrium condition,

[Downloaded from ase.iust.ac.ir on 2025-04-09]

[DOI: 10.22068/ase.2025.692]

International Journal of Heat and Mass Transfer, vol. 68, (2014), pp. 161-173.

[23] A. Mohamad, Heat transfer enhancements in heat exchangers fitted with porous media Part I: constant wall temperature, International journal of thermal sciences, vol. 42, no. 4,(2003), pp. 385-395.

[24] S. R. Hassan, T. Islam, M. Ali, and M. Q. Islam, Numerical study on aerodynamic drag reduction of racing cars, Procedia Engineering, vol. 90, (2014), pp. 308-313.

[25] D. Igali, O. Mukhmetov, Y. Zhao, S. C. Fok, and S. L. Teh, Comparative analysis of turbulence models for automotive aerodynamic simulation and design, International Journal of Automotive Technology, vol. 20, (2019), pp. 1145-1152.

[26] S. Chakchak, A. Hidouri, A. Ghabi, M. Chrigui, and T. Boushaki, Numerical Study of Turbulent Swirling Diffusion Flame Under Lean and Rich Conditions Using Turbulence Realizable k-epsilon Model, Combustion Science and Technology, vol. 195, no. 7, (2023), pp. 1461-1482.

[27] H. Saberinejad and A. Keshavarz, Reciprocating turbulent flow heat transfer enhancement within a porous medium embedded in a circular tube, Applied Thermal Engineering, vol. 102,(2016), pp. 1355-1365.

[28] W. Ehlers, "Darcy, Forchheimer, Brinkman and Richards: classical hydromechanical equations and their significance in the light of the TPM," Archive of Applied Mechanics, vol. 92, no. 2, (2022), pp. 619-639.

[29] Y. Yi, X. Bai, F. Kuwahara, and A. Nakayama, A local thermal non-equilibrium solution based on the brinkman–forchheimer-extended darcy model for thermally and hydrodynamically fully developed flow in a channel filled with a porous medium, Transport in Porous Media, vol. 139, (2021), pp. 67-88.

[30] A. Abderrahmane et al., Heat and mass transfer analysis of non-Newtonian power-law nanofluid confined within annulus enclosure using Darcy-Brinkman-Forchheimer model, Case Studies in Thermal Engineering, vol. 40, (2022), pp. 102569.

[31] R. Franzke, S. Sebben, T. Bark, E. Willeson, and A. Broniewicz, Evaluation of the multiple reference frame approach for the modelling of an axial cooling fan, Energies, vol. 12, no. 15, (2019), pp. 2934,.

[32] W. Peng, G. Li, J. Geng, and W. Yan, A strategy for the partition of MRF zones in axial fan simulation, International Journal of Ventilation, vol. 18, no. 1, (2019), pp. 64-78.

[Downloaded from ase.iust.ac.ir on 2025-04-09]

[DOI: 10.22068/ase.2025.692]